

CHARACTERIZATION AND GEOCHEMISTRY OF CARBONATE CAPROCK
ASSOCIATED WITH THE GYPSUM VALLEY SALT WALL, PARADOX
BASIN, COLORADO: IMPLICATIONS FOR UNDERSTANDING
LATERAL CAPROCK EMPLACEMENT

PIPER LEE POE

Master's Program in Geological Sciences

APPROVED:

Katherine A. Giles, Ph.D., Chair

Benjamin Brunner, Ph. D.

Eric E. Hiatt, Ph.D.

Charles Amber, Ph.D.
Dean of the Graduate School

Copyright ©

by

Piper Poe

2018

Dedication

To Dr. Eric Hiatt, who unknowingly put me on the road to find my passion for science.

PREVIEW

PREVIEW

CHARACTERIZATION AND GEOCHEMISTRY OF CARBONATE CAPROCK
ASSOCIATED WITH THE GYPSUM VALLEY SALT WALL, PARADOX
BASIN, COLORADO: IMPLICATIONS FOR UNDERSTANDING
LATERAL CAPROCK EMPLACEMENT

by

PIPER LEE POE, B.S. Geology

THESIS

Presented to the Faculty of the Graduate School of
The University of Texas at El Paso
in Partial Fulfillment
of the Requirements
for the Degree of

MASTER OF SCIENCE

Department of Geological Sciences
THE UNIVERSITY OF TEXAS AT EL PASO
December 2018

ProQuest Number: 13424563

All rights reserved

INFORMATION TO ALL USERS

The quality of this reproduction is dependent upon the quality of the copy submitted.

In the unlikely event that the author did not send a complete manuscript and there are missing pages, these will be noted. Also, if material had to be removed, a note will indicate the deletion.



ProQuest 13424563

Published by ProQuest LLC (2019). Copyright of the Dissertation is held by the Author.

All rights reserved.

This work is protected against unauthorized copying under Title 17, United States Code
Microform Edition © ProQuest LLC.

ProQuest LLC.
789 East Eisenhower Parkway
P.O. Box 1346
Ann Arbor, MI 48106 – 1346

Acknowledgements

This work would not have been accomplished without my advisor, Dr. Kate Giles. I thank her for her constant inspiration and enthusiasm, and the countless opportunities she provided me throughout this process. Her persistent confidence in my work and my abilities have allowed me to go farther than I thought possible. The love and excitement she has for geology is incredibly contagious and makes working with her an absolute pleasure.

The financial support from the sponsors of the Institute of Tectonic Studies Salt-Sediment Research Consortium at the University of Texas at El Paso provided the tools to complete this study. Current sponsors include ExxonMobil, Hess, BP, BHP-Billiton, Repsol, Total, Chevron, and Conoco Phillips. Additional funding from the Geological Society of America Research Grants, Geological Society of America Travel Grants, American Association of Petroleum Geologists Grants-In-Aid, American Association of Petroleum Geologists-Southwest Section, and the University of Texas at El Paso Dodson Research Grant provided funds for multiple geochemical analyses, to complete fieldwork in Colorado and to travel to the Dead Sea, Israel to present my research at the Penrose Conference.

The creation of this thesis would not have been possible without those who contributed their knowledge and expertise, including Dr. Ben Brunner, Dr. Eric Hiatt, Dr. Richard Langford, Evey Gannaway, Carl Fiduk, Dr. Mark Rowan, Dr. Chris Jackson, and Dr. Frank Peel. I thank Rachelle Kernen for the guidance, advise and the opportunities she provided throughout this process, and for trusting me to be a part of her work. I also want to thank my trusty field assistant and best friend, Rafael Delfin, for the great times and moral support that immensely contributed to the writing of this thesis. Finally, a special thanks to Nila Matsler for her great organization and refreshing conversation.

Abstract

On the northeastern side of Gypsum Valley salt wall in the Paradox Basin of Colorado, discontinuous exposures of layered gypsum and carbonate rocks were previously mapped as the contact between diapiric Paradox Formation and marine limestone of the Pennsylvanian Honaker Trail Formation. Utilizing new and existing mapping, petrographic and isotopic geochemical analyses, this study reinterprets this zone to represent lateral gypsum and carbonate caprock that formed in the Triassic during passive rise of the Gypsum Valley salt wall. Gypsum Valley lateral carbonate caprock can be distinguished from Pennsylvanian and Permian depositional carbonate strata exposed elsewhere on the salt wall by the recognition of caprock distinctive fabrics (i.e. massive, porphyritic, layered and brecciated), the lack of fossils or sedimentary structures, the lack of depositional interfingering with the adjacent outboard Triassic Chinle Formation stratigraphy, and its carbon isotopic signature ($< -6\text{‰}$) that reflects the contribution of isotopically light carbon from the oxidation of hydrocarbons during caprock formation. Additionally, the preliminary results from the lateral carbonate caprock produced a U-Pb age of $211 \pm 16\text{Ma}$, which is consistent with the upper Triassic age suggested by the association with the Chinle Formation. The orientation of the lateral caprock layering parallels that of the adjacent halokinetically drape-folded Chinle strata, which contains fluvial channel conglomerate-bearing, caprock-derived clasts. This confirms that the carbonate caprock had already formed in the Triassic in a crestal position on top of the Gypsum Valley salt wall during Chinle deposition and was subsequently rotated by halokinetic drape folding to its flanking position during continued passive diapirism.

In addition to the reinterpretation of the studied gypsum and carbonate units as lateral caprock, the term “capstone” was introduced when discussing a particular caprock lithology, as a distinction from the term “caprock” that is generally used in reference to the entire rock body. A

capstone classification is proposed based on the recognition of four distinct megascopic fabric types: 1) massive: consisting of a homogeneous mineralogy and texture; 2) porphyritic: comprising two distinct crystal sizes; 3) layered: subdivisions based on layer size that includes: microlaminated (1-3mm), laminated (3-10mm), and banded (>10mm); and 4) brecciated: these units are subdivided based on the degree of separation between brecciated capstone fragments, which may be close, loose, or spatially independent and subdivided into crackle breccia, mosaic breccia, and disorganized breccia, respectively. Paragenetic relationships indicate micritic dolomite to be the original carbonate capstone fabric formed during the Triassic. Thus, the additional capstone fabrics and mineralogies exposed today signify the diagenetic alteration of the original dolomite capstone, likely by multiple fluid flow events. Therefore, it is possible to use the evolution of capstone fabrics as an archive of fluid flow at the salt-sediment interface.

Table of Contents

Acknowledgements.....	v
Abstract.....	vi
Table of Contents.....	viii
List of Tables	xi
List of Figures.....	xii
Chapter 1: Introduction	1
1.1. Caprock Formation	1
1.2. Lateral Caprock.....	4
1.3. Significance.....	10
1.4. Research Objectives.....	11
1.5. Geologic Setting.....	12
1.6. Methods.....	16
Chapter 2: Fabric Classification of the Gypsum and Carbonate Caprock at the Gypsum Valley Salt Wall	22
2.1. Massive Capstone	23
2.1.1. Massive dolomite capstone	23
2.1.2. Massive Calcite Capstone	25
2.1.3. Massive Gypsum Capstone	25
2.2. Porphyritic Capstone.....	25
2.2.1. Porphyritic silica-dolomite capstone	28
2.2.2. Porphyritic silica-calcite capstone.....	28
2.2.3. Porphyritic calcite capstone.....	28
2.2.4. Porphyritic gypsum capstone	32
2.3. Layered Capstone.....	32
2.3.1. Microlaminated Capstone.....	34
2.3.1.1. Microlaminated Dolomite Capstone	34
2.3.1.2. Microlaminated Calcite Capstone.....	34
2.3.1.3. Microlaminated Gypsum Capstone.....	37
2.3.2. Laminated Capstone	37
2.3.2.1. Laminated Calcite Capstone	37
2.3.2.2. Laminated Dolomite Capstone	40

2.3.2.3. Laminated Silica-Dolomite Capstone	40
2.3.3. Banded Capstone	43
2.3.3.1. Banded Calcite-Dolomite Capstone.....	43
2.3.3.2. Banded Calcite Capstone	43
2.4. Brecciated Capstone.....	46
2.4.1. Crackle Breccia Capstone	46
2.4.1.1. Crackle Breccia Dolomite Capstone.....	46
2.4.2. Mosaic Breccia Capstone	48
2.4.2.1. Mosaic Breccia Dolomite Capstone.....	48
2.4.2.2. Mosaic Breccia Gypsum-Dolomite Capstone.....	48
2.4.3. Disorganized Breccia Capstone.....	51
2.4.3.1. Disorganized Breccia Dolomite Capstone.....	51
2.4.3.2. Disorganized Breccia Calcite Capstone.....	53
Chapter 3: Distribution of Capstone Fabrics Along the Gypsum Valley Salt Wall	55
3.1. The Nubbin	55
3.2. Box Canyon – Bridge Canyon.....	58
3.2.1. Box Canyon.....	58
3.2.1. Bridge Canyon.....	58
3.3. Mary Jane Draw	61
3.4. Carbonate Caprock Clasts.....	63
Chapter 4: Geochemical Observations of Gypsum Valley Carbonate Caprock	65
4.1. $\delta^{18}\text{O}$ versus $\delta^{13}\text{C}$ Cross-Plot: Carbonate Capstone Fabrics.....	65
4.2. $\delta^{18}\text{O}$ versus $\delta^{13}\text{C}$ Cross-Plot: Carbonate Capstone Petrographic Observations.....	69
4.3. Carbon and Oxygen Isotopic Signature of Carbonate Clasts Found within the Chinle Formation.....	70
4.4. U-Pb Age Dating of Carbonate Capstones	72
Chapter 5: Discussion	75
5.1. Interpretation of Capstone Fabrics.....	75
5.1.1. Massive Capstone.....	75
5.1.2. Porphyritic Capstone	75
5.1.3. Layered Capstone	76
5.1.4. Brecciated Capstone	77

5.2. Paragenesis of Capstone Fabrics.....	78
5.2.1. Paragenetic Relationships within Caprock.....	78
5.2.2. Controls on the Spatial Distribution of Capstone Fabrics.....	80
5.3. Geochemical Signature of Carbonate Capstone	82
5.3.1. Isotopically Low Carbon Signature of Carbonate Capstone	82
5.3.2. Diagenetic Overprinting of Complex Carbonate Capstone Fabrics	85
5.3.3. Geographic Distribution of Geochemical Signatures along the Gypsum Valley Salt Wall	86
5.3.4. Geochemical Signature of Carbonate Capstone Clasts within the Chinle Formation	88
5.3.5. U-Pb Age Dating of Carbonate Capstone	89
5.4. Hypotheses/Models for Lateral Caprock Emplacement.....	89
5.4.1. Pennsylvanian Honaker Trail Formation Hypothesis	90
5.4.2. Paradox LES Model	91
5.4.3. In-Situ Model	93
5.4.4. Halokinetic Drape-Fold Model	94
5.5. Chinle Caprock Formation by the Drape-Fold Model.....	95
Chapter 6: Conclusion.....	99
References.....	102
Curriculum Vita	106

List of Tables

Table 1: Classification of caprocks associated with salt diapirs according to fabric.....	23
Table 2: Comparison of the mean host and cement isotopic composition of capstone fabrics.....	67

PREVIEW

List of Figures

Figure 1: Crestal caprock	2
Figure 2.1: Anhydrite caprock formation	3
Figure 2.2: Carbonate caprock formation	3
Figure 3: Seismic and interpreted illustration of caprock at Epsilon diapir	5
Figure 4: <i>In-situ</i> lateral caprock model.....	6
Figure 5: Layered evaporite sequence (LES) model.....	6
Figure 6: Halokinetic drape-fold model.....	7
Figure 7: Regional location of Paradox Basin	9
Figure 8: Geologic map of the Gypsum Valley salt wall.....	14
Figure 9: Stratigraphic column of the Chinle Formation.....	15
Figure 10: Conceptual model of the Gypsum Valley salt shoulder.....	17
Figure 11: Geologic map of Gypsum Valley highlighting caprock location.....	19
Figure 12: Massive dolomite capstone	24
Figure 13: Massive calcite capstone	26
Figure 14: Massive gypsum capstone.....	27
Figure 15: Porphyritic silica-dolomite capstone.....	29
Figure 16: Porphyritic silica-calcite capstone.....	30
Figure 17: Porphyritic calcite capstone.....	31
Figure 18: Porphyritic gypsum capstone	33
Figure 19: Microlaminated dolomite capstone	35
Figure 20: Microlaminated calcite capstone.....	36
Figure 21: Microlaminated gypsum capstone.....	38
Figure 22: Laminated calcite capstone	39
Figure 23: Laminated dolomite capstone.....	41
Figure 24: Laminated silica-dolomite capstone.....	42
Figure 25: Banded calcite-dolomite capstone.....	44
Figure 26: Banded calcite capstone	45
Figure 27: Crackle breccia dolomite capstone.....	47
Figure 28: Mosaic breccia dolomite capstone	49
Figure 29: Mosaic breccia gypsum-dolomite capstone	50
Figure 30: Disorganized breccia dolomite capstone.....	52

Figure 31: Disorganized breccia calcite capstone.....	54
Figure 32: Geologic map of exposed capstone along the Gypsum Valley salt wall.....	56
Figure 33: Caprock fabric map of The Nubbin.....	57
Figure 34: Caprock fabric map of Box Canyon and Bridge Canyon.....	60
Figure 35: Caprock fabric map of Mary Jane Draw	62
Figure 36: Dolomite clasts within the Chinle Formation.....	64
Figure 37: $\delta^{18}\text{O}$ versus $\delta^{13}\text{C}$ cross-plot of exposed carbonate caprock at Gypsum Valley.....	66
Figure 38: $\delta^{18}\text{O}$ versus $\delta^{13}\text{C}$ cross-plot of carbonate capstone fabrics.....	68
Figure 39: $\delta^{18}\text{O}$ versus $\delta^{13}\text{C}$ cross-plot of mineral phases within carbonate capstone	71
Figure 40: Isochrons of U-Pb age dates of carbonate caprock	73
Figure 41: Carbonate caprock samples used for U-Pb age dating	74
Figure 42: Calcite capstone replacement of micritic dolomite capstone	79
Figure 43: $\delta^{18}\text{O}$ versus $\delta^{13}\text{C}$ cross-plot of primary carbonate capstone fabrics	84
Figure 44: $\delta^{18}\text{O}$ and $\delta^{13}\text{C}$ versus distance from the Nubbin.....	87
Figure 45: $\delta^{18}\text{O}$ versus $\delta^{13}\text{C}$ cross-plot of all carbonates exposed at Gypsum Valley.....	92
Figure 46: Conceptual illustration of the Gypsum Valley salt shoulder development.....	96
Figure 47: Schematic illustration of the caprock exposed over the modern salt shoulder	97

Chapter 1: Introduction

1.1. Caprock Formation

Caprocks associated with salt diapirs are mineral assemblages formed as salt dissolution-related insoluble residues (Murray, 1966; Kyle et al., 1987) that are typically found on the diapir crest, and occasionally in a flanking position, where they are referred to as lateral caprock (Jackson and Lewis, 2012). Caprock assemblages commonly consist of a vertically zoned layered sequence, containing in ascending order: anhydrite, gypsum, and carbonate lithologies such as limestone and dolostone (Kyle and Posey, 1991) (Figure 1). The formation of the anhydrite/gypsum caprock involves a cross-flow of halite-undersaturated phreatic water to the diapir, which causes the halite in the salt diapir to preferentially dissolve from the rising diapir. As the halite dissolves, the less soluble components of the diapir, such as CaSO_4 minerals (i.e. anhydrite and gypsum) accumulate as insoluble residues and accrete to the base of the developing caprock by underplating (Kyle et al., 1987; Kyle and Posey, 1991) (Figure 2.1). The formation of carbonate caprocks involves the alteration of CaSO_4 minerals by bacterially controlled diagenetic processes (Kyle et al., 1987). This occurs in a two-stage process: first, fluids dissolve CaSO_4 from the anhydrite caprock, releasing Ca^{2+} and SO_4^{2-} to solution; second, if in the presence of sulfate-reducing bacteria and organic matter, sulfate is reduced and hydrocarbons are oxidized, releasing bicarbonate and hydrogen sulfide as a result. The bicarbonate in solution bonds with calcium to precipitate calcite, and if magnesium is present, dolomite precipitates, producing a carbonate caprock (Figure 2.2) (Hallager et al., 1990; Kyle and Posey, 1991; Warren, 2006).

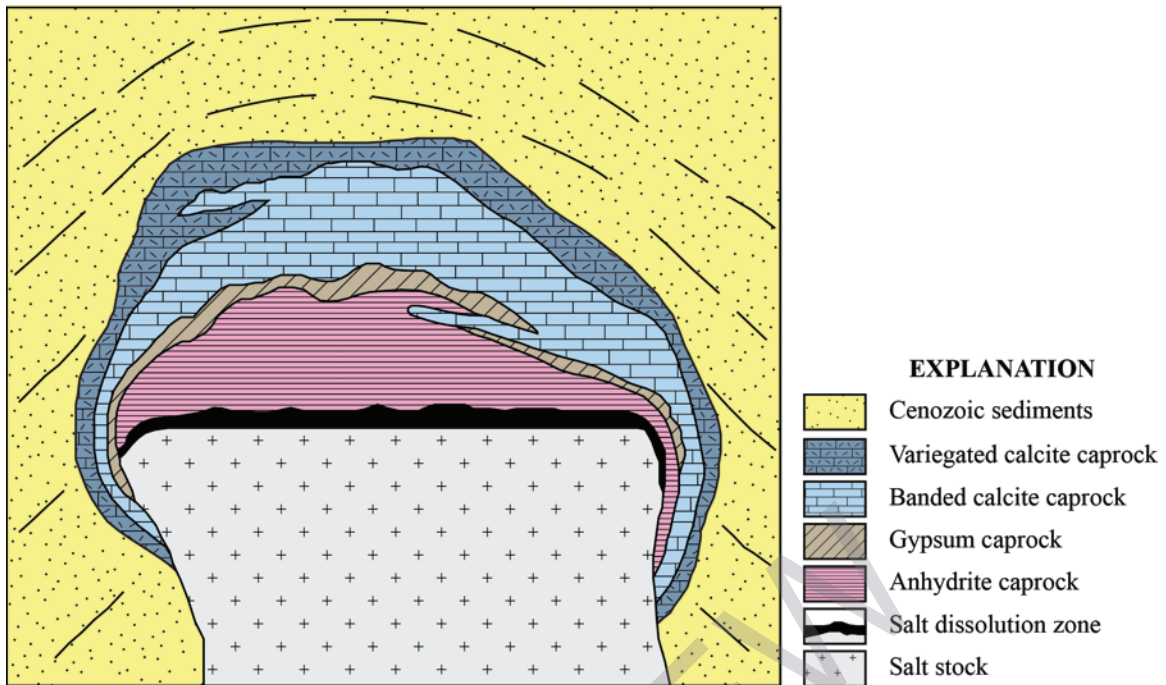


Figure 1. Cross sectional view of a Texas Gulf Coast salt dome showing generalized caprock lithologic zonation. Modified from Kyle and Posey, 1991.

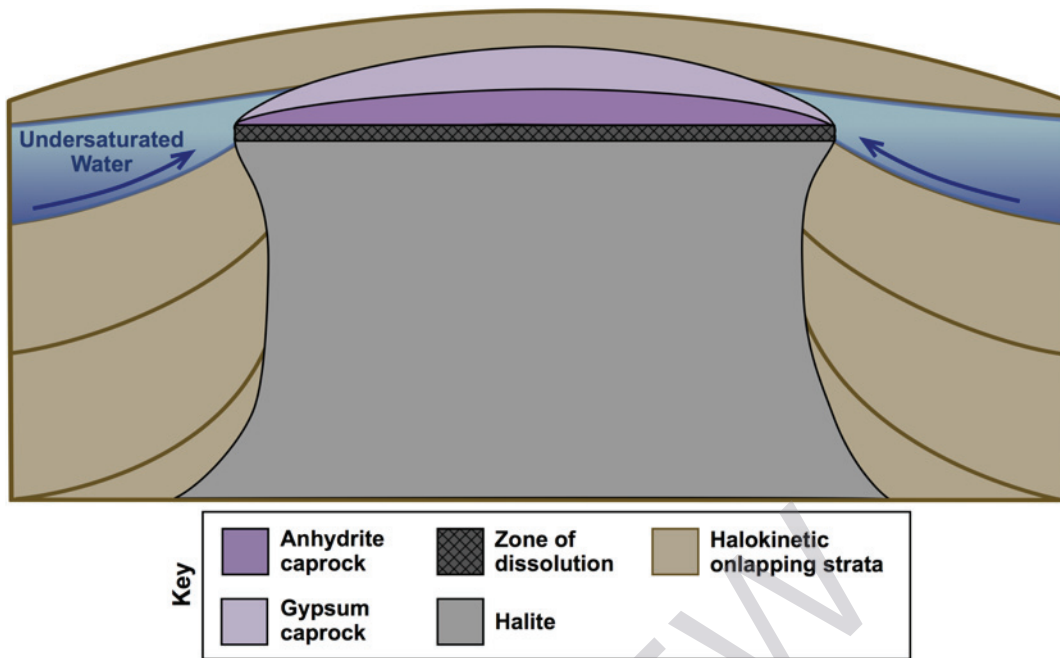


Figure 2.1. Schematic diagram of anhydrite/gypsum caprock formation. No scale implied.

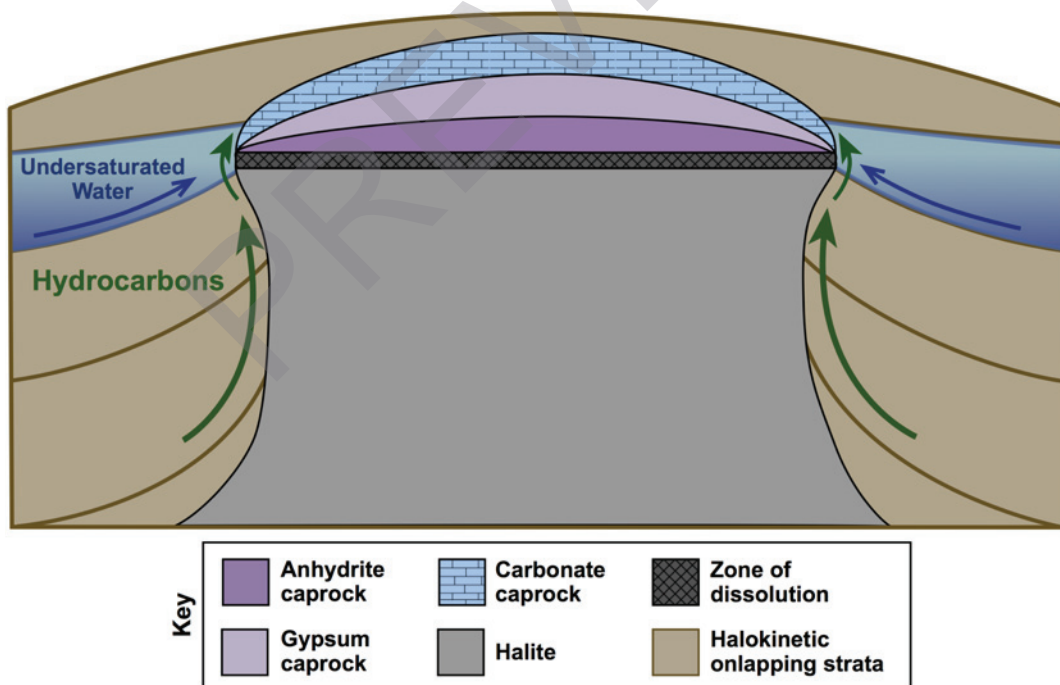


Figure 2.2. Schematic diagram of carbonate caprock formation. No scale implied.

1.2. Lateral Caprock

Lateral caprock has been identified at the Epsilon Diapir in the North Sea Egersund Basin (Jackson, et al., 2013) and at the Hockley, Boling, and Moss Bluff salt domes in the Texas Gulf Coast (Kyle and Posey, 1991) in diapir-flanking positions hundreds of meters in the subsurface (Figure 3). Currently, three general models have been proposed for the formation of lateral caprock: 1) *in-situ* model, 2) rotated layered evaporite sequence model, and 3) halokinetic drape fold (“event”) model. The *in-situ* model, proposed by Evans et al. (1991), suggests that emplacement of lateral caprock is the result of unusual undersaturated deeply circulating basinal waters that flow upward along the flanks of the diapir. The outward dipping geometries of the surrounding strata assist the buoyancy-driven flow that then preferentially dissolves halite and accretes CaSO_4 minerals resulting in lateral caprock development (Figure 4) (Evans, 1991; Jackson, et al., 2013). The rotated layered evaporite sequence (LES) model, proposed by Schwerdthier et al. (1978), suggests that a depositional/early post-depositional anhydrite-dominated evaporite sequence associated with the autochthonous depositional salt strata has been rotated upward to a position against the flank of the diapir during diapiric rise (Figure 5). Giles et al. (2012), suggest that lateral caprock initially forms in a roughly horizontal position on the crest of a diapir and is subsequently rotated to the lateral position by halokinetic drape-folding of the coupled caprock and roof strata during continued passive diapiric rise. The lateral caprock is associated with a discrete package of roof strata. Thus, the formation age of the caprock should be roughly equivalent to that of the adjacent halokinetically deformed strata. Giles et al. (2012) refers to this process as a “caprock event” (Figure 6), and a single passive diapir may have multiple caprock events. In contrast, existing models of crestal caprock formation envision caprock

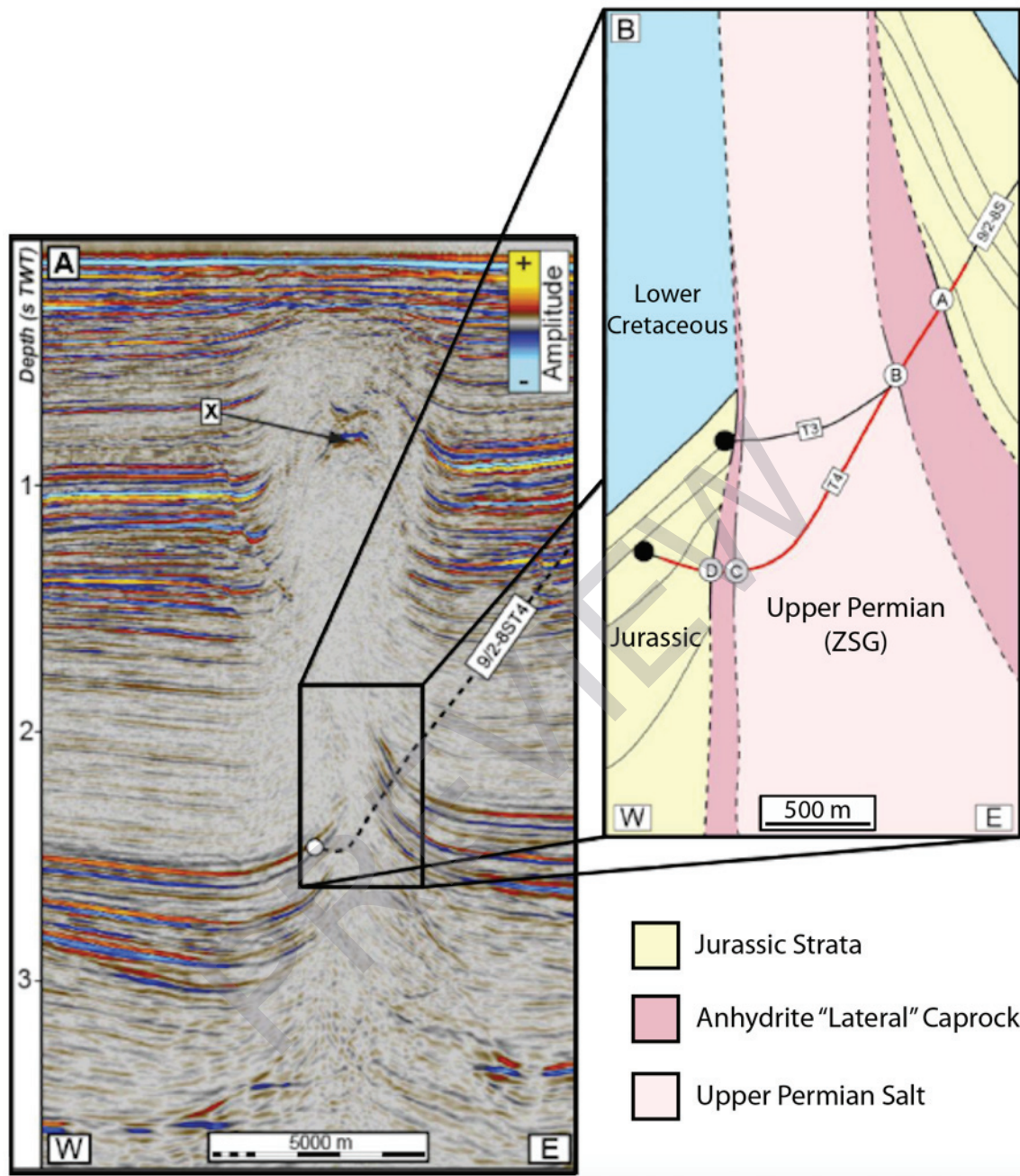


Figure 3. A. Seismic reflection, B. Seismic interpretation of the Epsilon Diapir in the Egarsund Basin, North Sea. Well 9/2-8S penetrated anhydrite caprock along the flanks of the Epsilon Diapir while drilling a Jurassic prospect (Jackson, C. A., et al, 2013).

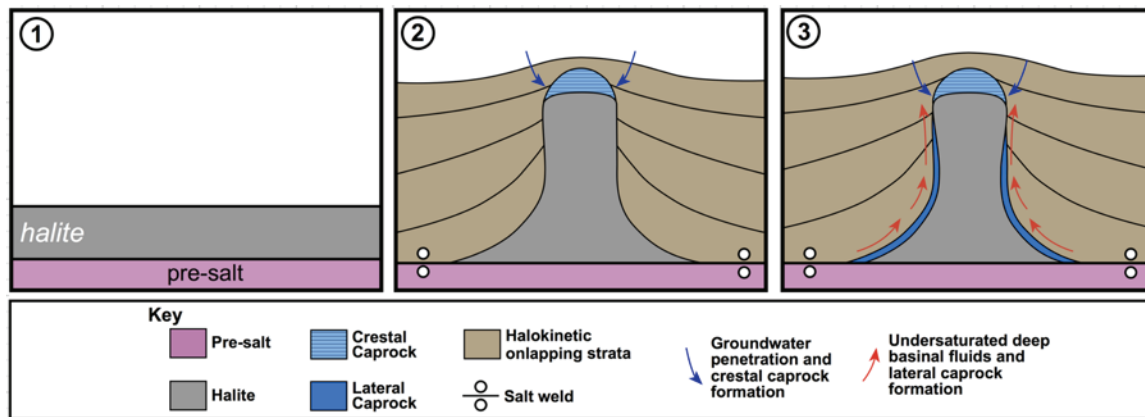


Figure 4. Conceptual model representing the *in-situ* model of lateral caprock as a mode of lateral caprock emplacement, proposed by Jackson and Lewis (2012). The model proposes that lateral caprock forms as a result of migration of undersaturated basinal fluid migration along the diapir flank. Modified from Jackson and Lewis, 2012.

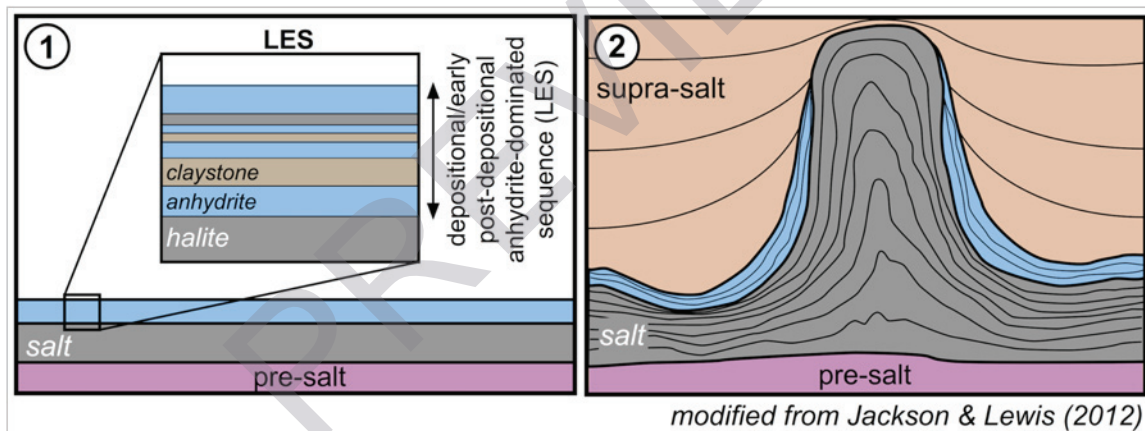


Figure 5. Simplified diagram illustrating the layered evaporite sequence (LES) model, proposed by Schwerdther et al. (1978) suggests that lateral caprock could essentially be a LES associated with the mother salt that has been plastered against the flank of the diapir during the rise of less dense halite. No scale is implied. Modified from Jackson and Lewis, 2012.

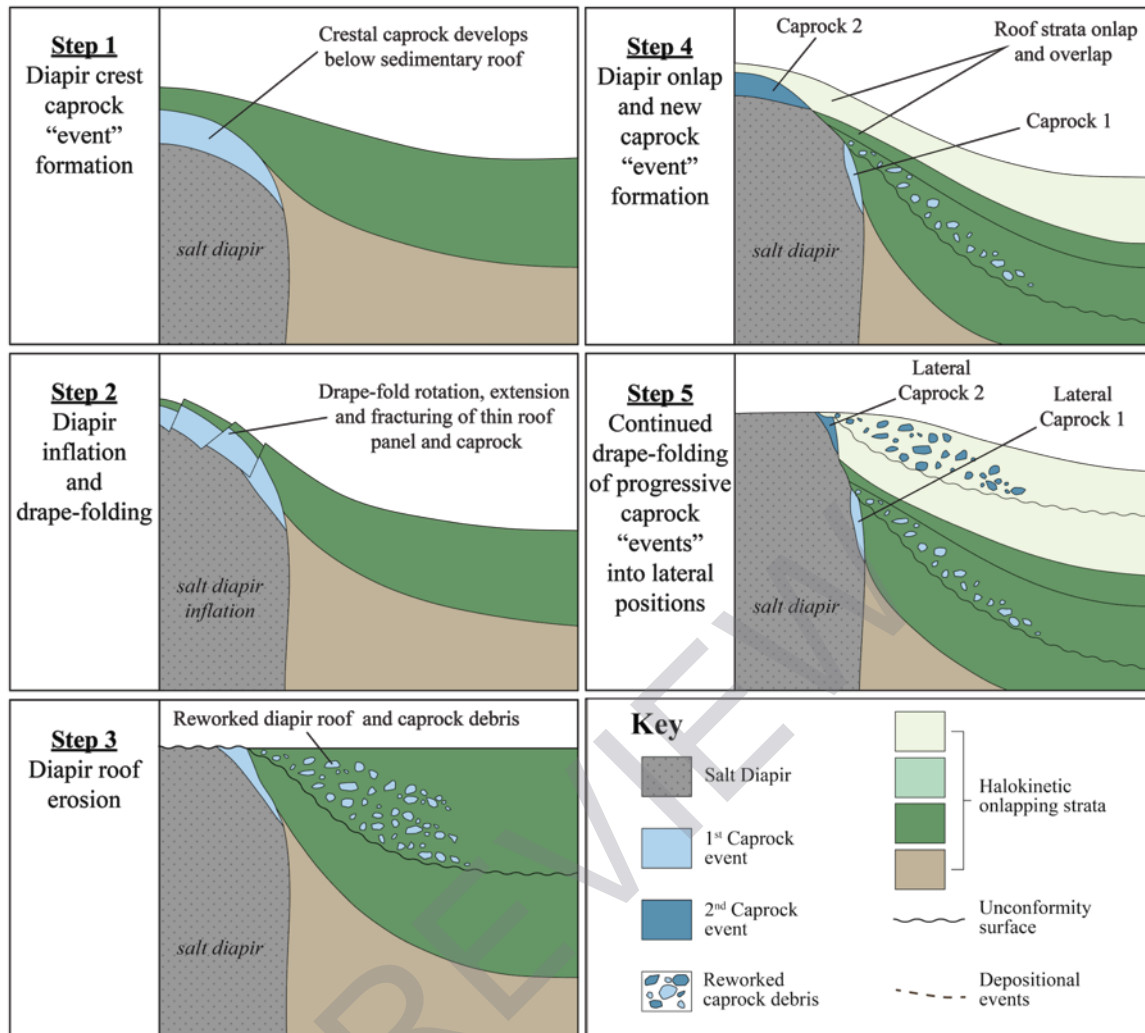


Figure 6. Conceptual diagram illustrating the halokinetic drape-fold model proposed by Giles et al. (2012) for a mode of lateral caprock emplacement, which suggests caprock forms in a crestal position during distinct periods of time and are then rotated into a lateral position as a result of halokinetic drape folding. No scale is implied. Modified from Giles et al., 2012.

generation by long-lived, crestal dissolution of halite with the caprock rising continuously along with salt during ongoing diapirism (Murray, 1966; Kyle and Posey, 1991).

The halokinetic drape-fold event model consists of four steps: 1) caprock develops in a crestal position by cross-flow of undersaturated waters; 2) continued diapiric rise and minibasin subsidence causes drape-folding of roof strata and competent caprock, which detaches from the underlying halite-dominated diapir and rotates off the crest into a lateral position; 3) topography generated by diapir inflation as diapir-rise rates exceed sedimentation rates results in erosional thinning of the roof to create an angular unconformity that truncates the underlying lateral caprock and potential incorporation of caprock clasts into the surrounding sediments; 4) increasing rates of sedimentation relative to diapiric rise lead to onlap and formation of the overlying halokinetic sequence, which may or may not develop a new crestal caprock assemblage (Giles et al., 2012).

Shock (2012) established the applicability of the halokinetic drape fold model as the mode of emplacement for the Permian Cutler Formation-age equivalent lateral caprock found at the margin of Castle Valley salt wall, Paradox Basin, Utah (Figure 7). Here, vertical layers of dolomitic and calcitic caprock separate the massive gypsum exposures of the Castle Valley salt wall from vertical to overturned strata of the Permian Cutler Formation. Fluvial channel conglomeratic facies in this Cutler strata contain caprock-derived clasts (Shock, 2012). Recently, lateral gypsum and carbonate caprock has also been documented at the Gypsum Valley salt wall in the Paradox Basin, CO, (Figure 7) (McFarland, 2016; Brunner et al., 2016; Lerer, 2017), where it is associated with 25 degree NE dipping strata of the Triassic Chinle Formation (Figure 8). McFarland (2016) and Heness *et al.* (2017) interpret carbonate clasts in the fluvial conglomerate facies to be derived from the caprock. Carbonate caprock clasts found in the halokinetic sequence of the overlying Triassic Chinle Formation are essential pieces of evidence supporting the drape

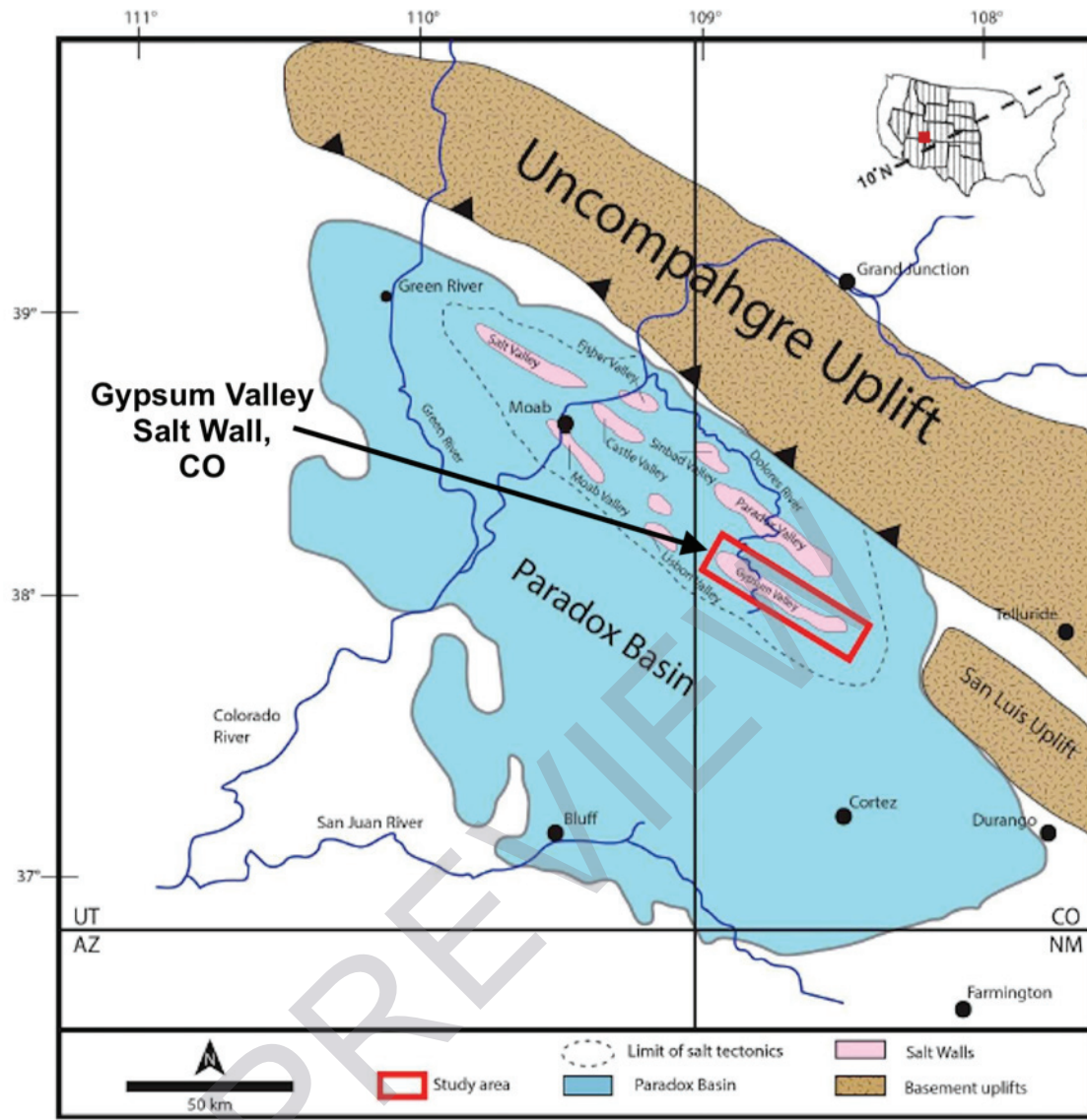


Figure 7. Location map of Paradox Basin and salt anticline province showing major uplifts and salt anticlines. Gypsum Valley salt wall study area is outlined in red. (modified from Barbeau, 2003; and Kues and Giles, 2004).